


RESEARCH

Open Access

PET imaging of mGluR5 in Alzheimer's disease



Adam P. Mecca^{1,2}, Julia W. McDonald^{1,2}, Hannah R. Michalak^{1,2}, Tyler A. Godek^{1,2}, Joanna E. Harris^{1,2}, Erika A. Pugh^{1,2}, Emily C. Kemp^{1,2}, Ming-Kai Chen⁵, Arash Salardini⁴, Nabeel B. Nabulsi⁵, Keunpoong Lim⁵, Yiyun Huang⁵, Richard E. Carson⁵, Stephen M. Strittmatter^{3,4,6*} and Christopher H. van Dyck^{1,2,3,4*} 

Abstract

Background: Metabotropic glutamate subtype 5 receptors (mGluR5) modulate synaptic transmission and may constitute an important therapeutic target in Alzheimer's disease (AD) by mediating the synaptotoxic action of amyloid- β oligomers. We utilized the positron emission tomography (PET) radioligand [¹⁸F]FPEB to investigate mGluR5 binding in early AD.

Methods: Sixteen individuals with amnesic mild cognitive impairment (MCI) due to AD or mild AD dementia who were positive for brain amyloid were compared to 15 cognitively normal (CN) participants who were negative for brain amyloid. Diagnostic groups were well balanced for age, sex, and education. Dynamic PET scans were acquired for 60 min, starting at 60 min after the initial administration of up to 185 MBq of [¹⁸F]FPEB using a bolus-plus-constant-infusion method (K_{bol} = 190 min). Equilibrium modeling with a cerebellum reference region was used to estimate [¹⁸F]FPEB binding (BP_{ND}) to mGluR5. Analyses were performed with and without corrections for gray matter atrophy and partial volume effects.

Results: Linear mixed model analysis demonstrated a significant effect of group ($p = 0.011$) and the group \times region interaction ($p = 0.0049$) on BP_{ND} . Post hoc comparisons revealed a significant reduction (43%) in mGluR5 binding in the hippocampus of AD ($BP_{ND} = 0.76 \pm 0.41$) compared to CN ($BP_{ND} = 1.34 \pm 0.58$, $p = 0.003$, unpaired t test) participants, and a nonsignificant trend for a reduction in a composite association cortical region in AD ($BP_{ND} = 1.57 \pm 0.25$) compared to CN ($BP_{ND} = 1.86 \pm 0.63$, $p = 0.093$) participants. Exploratory analyses suggested additional mGluR5 reductions in the entorhinal cortex and parahippocampal gyrus in the AD group. In the overall sample, hippocampal mGluR5 binding was associated with episodic memory scores and global function.

Conclusions: [¹⁸F]FPEB-PET revealed reductions in hippocampal mGluR5 binding in early AD. Quantification of mGluR5 binding in AD may expand our understanding of AD pathogenesis and accelerate the development of novel biomarkers and treatments.

Keywords: mGluR5, Glutamate receptor, Alzheimer's disease, [¹⁸F]FPEB, PET

Introduction

Metabotropic glutamate subtype 5 receptors (mGluR5) are seven-transmembrane G protein-coupled receptors located in excitatory synapses [1] and in glial cells [2]. They are distributed throughout the cortex and hippocampus

where they modulate synaptic transmission [3, 4]. In rat brain, they are localized primarily postsynaptically [5, 6], but also presynaptically [7]. In primate prefrontal cortex, a substantial proportion are presynaptic [8]. In preclinical models of AD, mGluR5 has been hypothesized to mediate amyloid- β oligomer (A β) toxicity via several mechanisms, including promoting the clustering of A β as an extracellular scaffold for mGluR5 [9] and serving as a co-receptor for A β bound to cellular prion protein (PrP^C) for postsynaptic activation of the tyrosine kinase Fyn [10, 11].

* Correspondence: Stephen.strittmatter@yale.edu;
christopher.vandyck@yale.edu

³Department of Neuroscience, Yale University School of Medicine, New Haven, CT, USA

¹Alzheimer's Disease Research Unit, Yale University School of Medicine, One Church Street, 8th Floor, New Haven, CT 06510, USA

Full list of author information is available at the end of the article



mGluR5 may also link A β pathology to tau pathology in AD [12]. Complexes of A β and PrP^c create a hydrogel phase that recruits mGluR5 [13], leading to activation of the tyrosine kinase Fyn [10]. This activation of Fyn leads to downstream tau phosphorylation [14]. Furthermore, functional tau is required for postsynaptic targeting of Fyn and subsequent excitotoxicity mediated by NMDA receptors [15]. The absence of functional tau prevents memory deficits and premature death in transgenic APP23 mice that develop A β plaques [15].

Recognition of mGluR5 as a mediator of AD pathology and a potentially important therapeutic target [16] has stimulated the investigation of mGluR5 expression and receptor binding in AD models. Two studies have measured mGluR5 changes in mouse models of AD using positron emission tomography (PET). Fang et al. investigated mGluR5 in A β PP transgenic mice (tg-ArcSwe) using [¹¹C]ABP688-PET and reported no difference in binding compared to wild-type mice [17]. However, mGluR5 protein levels were increased in tg-ArcSwe mice when assessed with immunoblot. In a similar study, Lee et al. measured mGluR5 density in 5xFAD mice using [¹⁸F]FPEB-PET and immunoblot and observed lower mGluR5 binding and protein levels in the hippocampus and striatum compared to wild-type mice [18]. To our knowledge, no previous studies have investigated changes in mGluR5 receptor binding in living humans with AD.

In the present study, we utilized the PET radioligand [¹⁸F]FPEB to investigate mGluR5 binding in AD. To maximize statistical power in the setting of multiple regional comparisons, in our primary analyses, we focused on the hippocampus. This decision was based on post-mortem [19, 20] and in vivo [21] evidence of early synaptic loss in this region in AD, as well as mGluR5 reductions in AD model mice [18]. We also examined a composite association cortical region, given the evidence for selective vulnerability of association cortex in AD [22, 23]. We hypothesized that mGluR5 binding in the hippocampus and association cortex would be reduced in AD compared to CN participants. Further exploratory analyses were conducted to determine whether mGluR5 binding was reduced in a wider range of regions. Finally, we examined the associations between mGluR5 binding in the hippocampus or association cortex with episodic memory performance and global function.

Methods

Study participants and design

Participants between 55 and 85 years old underwent a screening diagnostic evaluation to ensure eligibility. Individuals with AD dementia were required to meet diagnostic criteria for probable dementia due to AD according to the National Institute on Aging–

Alzheimer's Association [24], have a Clinical Dementia Rating (CDR) score of 0.5 to 1.0 points, and a Mini-Mental Status Examination (MMSE) score of 16 to 26 points, inclusive. Participants with MCI were required to meet research diagnostic criteria for amnesic MCI [25], have a CDR score of 0.5 points, and a MMSE score of 24 to 30 points, inclusive. Both participants with AD dementia and MCI were required to have impaired episodic memory as evidenced by a Logical Memory II (LMII) score of 1.5 standard deviations below an education-adjusted norm. Participants who were cognitively normal were required to have a CDR score of 0, a MMSE score greater than 26, and a normal education-adjusted LMII score. The Rey Auditory Verbal Learning Test (RAVLT) was also administered to generate an episodic memory score. All participants received a PET scan with [¹¹C] Pittsburgh Compound B ([¹¹C]PiB) to determine the presence of brain amyloid- β accumulation. The [¹¹C]PiB PET scan was considered positive if both visual and quantitative criteria were met. Visual criteria entailed consensus of 2 experienced readers (APM and M-KC), and quantitative criteria required a [¹¹C]PiB cerebral-to-cerebellar distribution volume ratio (DVR) of 1.40 or more in at least 1 AD-affected region of interest (ROI) [26]. The study protocol was approved by the Yale University Human Investigation Committee and Radiation Safety Committee. All participants provided written informed consent prior to participating in the study.

Magnetic resonance imaging

Magnetic resonance imaging (MRI) was performed on a 3T Trio (Siemens Medical Systems, Erlangen, Germany) with a circularly polarized head coil. MRI acquisition consisted of a Sag 3D magnetization-prepared rapid gradient-echo (MPRAGE) sequence with 3.34-msec echo time, 2500-msec repetition time, 1100-msec inversion time, 7° flip angle, and 180 Hz/pixel bandwidth. Images are 256 × 256 × 176 with a pixel size of 0.98 × 0.98 × 1.0 mm. The MRI ensured that patients did not show evidence of infection, infarction, or other brain lesions. In addition, the MRI was used to define anatomy, to evaluate atrophy, and to perform partial volume correction (PVC).

Positron emission tomography

Acquisition and reconstruction

PET scans were performed on the HRRT (207 slices, resolution < 3 mm full width half maximum), the highest resolution human PET scanner [27]. List-mode data were reconstructed using the MOLAR algorithm [28] with event-by-event motion correction based on an optical detector (Vicra, NDI Systems, Waterloo, Canada) [29].

Dynamic [^{11}C]PiB scans were acquired for 90 min following administration of up to 555 MBq of tracer [30]. Dynamic [^{18}F]FPEB scans were acquired for 60 min, starting at 60 min after the initial administration of up to 185 MBq of tracer using a bolus/infusion method ($K_{\text{bol}} = 190$ min) [31].

Image co-registration and MRI segmentation

Software motion correction was applied to the dynamic PET images using a mutual-information algorithm (FSL-FLIRT) to perform frame-by-frame registration to a summed image (60–70 min). A summed motion corrected PET image was registered to the participant's MRI. The individual's MRI was nonlinearly registered to a template MRI to obtain regions of interest (ROIs) defined in the automated anatomical labeling (AAL) template [32]. A full description of the ROIs can be found in Additional file 1. Transformations were performed with Bioimagesuite (version 2.5; www.bioimagesuite.com). MR images were segmented into gray matter (GM), white matter (WM), and cerebrospinal fluid (CSF) using FAST-FMRIB's Automated Segmentation Tool (The Analysis Group, FMRIB, Oxford, UK). GM masking was performed by restricting ROIs using the GM segmentation mask.

Partial volume correction

PVC was performed using the Müller-Gärtner approach [33], according to previously described procedures [30]. Binary mask images of GM and WM were smoothed to the system resolution (~ 3 mm). For each dynamic PET frame, GM voxels were corrected for spill-in and spill-out of activity, assuming activity in CSF was zero and WM activity was uniform and was estimated from each image time frame.

Tracer kinetic modeling

For [^{11}C]PiB image analysis, parametric images of binding potential (BP_{ND}), the ratio at equilibrium of specifically bound radioligand to that of nondisplaceable radioligand in tissue [34], were generated using SRTM2 [35] with whole cerebellum as the reference region. BP_{ND} was calculated so that a value of 0 reflects no specific binding, i.e., tracer uptake no greater than that in the reference region. This is directly related to the DVR reported by other investigators [26], in that $DVR = BP_{\text{ND}} + 1$.

For [^{18}F]FPEB image analysis, parametric images of BP_{ND} were generated using equilibrium methods [36] with PET data collected from 90 to 120 min postinjection and whole cerebellum reference region [31, 37]. Three sets of BP_{ND} values were extracted: (1) uncorrected BP_{ND} using the full AAL region, (2) uncorrected BP_{ND} from the AAL region masked only to include GM voxels, and (3) PVC BP_{ND} , again with GM masking. We have previously evaluated a bolus plus constant infusion paradigm for

equilibrium modeling of both the distribution volume (V_T) and BP_{ND} for [^{18}F]FPEB [31, 38] and demonstrated excellent test-retest reproducibility for both parameters [31]. Although a validated reference region is not available for mGluR5-specific radioligands [39], the estimation of BP_{ND} using a region with a small amount of specific binding may be useful with certain assumptions and limitations (see the “Discussion” section). One such assumption is that the specific binding in the reference region does not differ between diagnostic groups. In support of this assumption, we also compared V_T in whole cerebellum between our AD and CN groups. V_T was calculated as the tissue-to-plasma radioactivity ratio at equilibrium (90–120 min postinjection) and reflects total uptake (specific plus nonspecific binding).

Whole brain PET and volumetric MRI analyses

Cortical reconstruction and volumetric segmentation were performed using Freesurfer (version 6.0, <http://surfer.nmr.mgh.harvard.edu/>) [40]. GM volume was normalized using estimated total intracranial volume [41]. For [^{18}F]FPEB image analysis, Freesurfer was used to co-register the parametric BP_{ND} image to the MRI for each subject. [^{18}F]FPEB BP_{ND} images were then sampled to the cortical surface and spatially smoothed using a 10 mm FWHM gaussian kernel.

Statistical analyses

Statistical analyses were performed using SPSS version 21.0 (IBM Corp.) or Matlab R2015a Statistics Toolbox (Mathworks, Inc.). Primary analyses utilized linear mixed models to compare mGluR5 binding (BP_{ND}) in the hippocampus and composite association cortex (within-participant factor) between AD and CN groups. The best-fitting variance-covariance structure, as determined by Bayesian information criterion, was compound symmetry. Secondary analyses utilized a similar model with exploratory regions listed in Table 2. Post hoc comparisons utilized unpaired t tests. To evaluate the contribution of GM tissue loss to mGluR5 reductions in AD, group differences in regional BP_{ND} after GM masking or PVC, as well as in regional GM volume, were also assessed using unpaired t tests. Additional exploratory analyses examined the relationships between hippocampal or association cortical BP_{ND} and episodic memory (average z -scores for LMII and RAVLT) and global function (CDR sum of boxes [CDR-SB]) in the combined sample with Pearson's correlation. Tests were two-tailed and used $p < 0.05$ as a threshold for significance. Vertex-wise, whole cortical analyses were performed with general linear models using Freesurfer. Permutation was used to correct for multiple comparisons. The cluster-forming threshold was $p < 0.01$, and the cluster-wise threshold was $p < 0.05$.

Results

Participant characteristics

The study sample consisted of 31 participants—16 with amnesic MCI due to AD or mild AD dementia and 15 who were CN. Diagnostic groups were well balanced for age, sex, and education, and both groups were highly educated (Table 1). AD participants had clinical characteristics typical of amnesic MCI and mild AD dementia with MMSE = 24.6 ± 4.3 and CDR-global = 0.72 ± 0.26 .

mGluR5 binding in Alzheimer's disease compared to cognitively normal participants

All participants received one injection of [^{18}F]FPEB (172 ± 21 MBq) with no significant difference in radioactivity (unpaired t test, $p = 0.132$) or mass dose (unpaired t test, $p = 0.412$) between groups. We observed no difference in whole cerebellar V_T from 90 to 120 min postinjection between AD (9.3 ± 1.8) and CN (8.6 ± 2.2) groups (unpaired t test, $p = 0.309$), supporting the use of cerebellum as the reference region in BP_{ND} calculations. Therefore, analyses were performed using parametric images normalized to whole cerebellum at equilibrium. Representative images of mGluR5 binding (BP_{ND}) indicate receptor availability throughout the cortex and in subcortical structures (Fig. 1a). Linear mixed model analysis, including group (CN, AD), region (hippocampus, association cortex), and the group \times region interaction as predictors, demonstrated a significant effect of group ($F(1, 31) = 7.4$, $p = 0.011$) and group \times region ($F(1, 31) = 9.2$, $p = 0.0049$) on BP_{ND} . Consistent with our hypothesis, we found a significant reduction (43%) in BP_{ND} in the hippocampus in AD (0.76 ± 0.41) compared to CN (1.34 ± 0.58) participants ($p = 0.003$, unpaired t test, Fig. 1b). However, we observed only a nonsignificant trend in mGluR5 binding in the association cortex between AD (1.57 ± 0.25) and CN (1.86 ± 0.63) participants ($p = 0.093$, unpaired t test, Fig. 1c).

Table 1 Participant characteristics and test results

	Cognitively normal	Alzheimer's disease
Participants (n)	15	16 (mild dementia, 8; MCI, 8)
Sex (M/F)	6/9	7/9
Age (years)	71.5 (8.4) (59–84)	73.1 (5.7) (63–82)
Education (years)	17.1 (2.3) (12–20)	16.7 (2.5) (12–20)
CDR-global	0 (0)	0.72 (0.26) (0.5–1)
CDR-SB	0 (0)	3.9 (2.2) (0.5–9.0)
MMSE	29.2 (1.2) (27–30)	24.6 (4.3) (17–29)
LMII	13.7 (3.8) (5–19)	1.9 (2.5) (0–7)
RAVLT-delay	11.7 (2.9) (4–15)	1.6 (2.5) (0–7)

Data are mean (SD) (range). CDR-global Clinical Dementia Rating global score, CDR-SB Clinical Dementia Rating sum of boxes, MMSE Mini-Mental State Examination, LMII Logical Memory II score, RAVLT Rey Auditory Verbal Learning Test

A secondary linear mixed model analysis explored the effect of diagnostic group (AD, CN) on mGluR5 binding (BP_{ND}) in a wider range of brain regions (Table 2). This analysis yielded a significant effect of group \times region ($F(11, 82) = 2.38$, $p = 0.013$), but not group ($F(1, 29) = 3.50$, $p = 0.072$). Post hoc analyses showed significant reductions of mGluR5 (BP_{ND}) in the entorhinal cortex (34% reduction, $p = 0.002$) and parahippocampal gyrus (26% reduction, $p = 0.012$) of AD participants (Table 2, unpaired t test, uncorrected for multiple comparisons).

Corrections for gray matter atrophy and partial volume effect

To evaluate the contribution of GM tissue loss to mGluR5 reductions in AD, we performed GM masking and PVC (Table 3). Hippocampal mGluR5 binding remained significantly lower in AD than in CN participants with GM masking ($BP_{ND} = 1.30 \pm 0.33$ vs. 1.78 ± 0.61 , $p = 0.011$) and PVC ($BP_{ND} = 2.19 \pm 0.45$ vs. 2.69 ± 0.88 , $p = 0.0499$). For the exploratory regional analyses, the reduction in mGluR5 remained significant after GM masking in the entorhinal cortex, but not in the parahippocampal gyrus. However, neither region retained significance after PVC (Table 3). This stepwise reduction in effect size with application of GM masking and PVC is consistent with both a dilution effect (i.e., as atrophy increases, GM volume within a region decreases) and a partial volume effect of GM atrophy on mGluR5 binding. To further elucidate these effects, we also performed a volumetric MRI analysis to assess GM volume differences between groups. This analysis demonstrated significant reductions in GM volume in the AD participants that were largest in the hippocampus and entorhinal cortex, but also present in the composite association cortex, parahippocampal gyrus, lateral temporal cortex, posterior cingulum, and occipital cortex (Additional file 1: Table S1).

Association between mGluR5 binding and episodic memory performance and global function

Pearson's correlations were performed to assess the relationship between mGluR5 binding and clinical assessments. Statistically significant correlations were found between hippocampal BP_{ND} and CDR-SB ($r = -0.53$, $p = 0.002$) and episodic memory performance ($r = 0.40$, $p = 0.027$; Fig. 2). No significant correlations were observed between association cortical BP_{ND} and CDR-SB ($r = -0.27$, $p = 0.143$) or episodic memory performance ($r = 0.14$, $p = 0.451$).

Whole brain analyses of mGluR5 binding

Further exploratory analyses were performed to compare mGluR5 binding in AD and CN participants for both the whole cortex (surface-based approach) and all

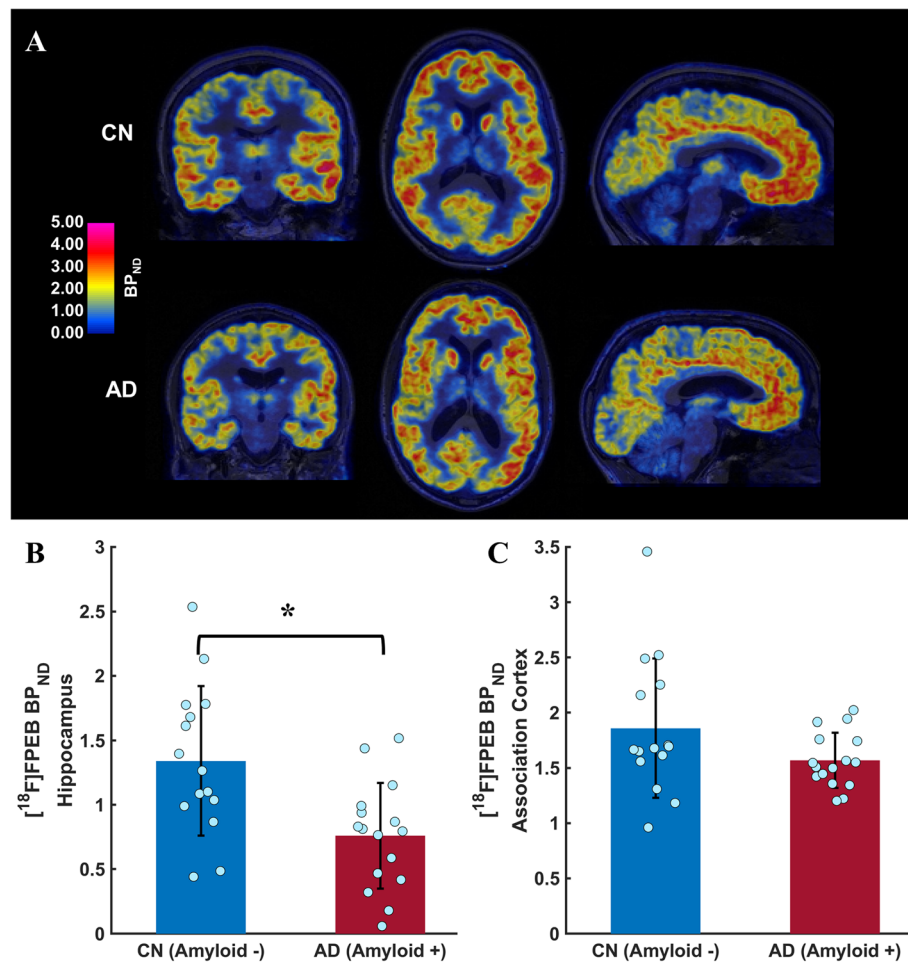


Fig. 1 mGluR binding ($[^{18}\text{F}]\text{FPEB } BP_{\text{ND}}$) in AD and CN participants measured with $[^{18}\text{F}]\text{FPEB}$ -PET. **a** Coronal, axial, and sagittal images of $[^{18}\text{F}]\text{FPEB}$ parametric PET (BP_{ND}) overlaid with T1 MRI scans in a representative CN (top row) and AD (bottom row) participant. The pseudocolor in PET images represents the intensity of $[^{18}\text{F}]\text{FPEB}$ binding (BP_{ND}). Reductions of $[^{18}\text{F}]\text{FPEB}$ binding are most noticeable in the medial temporal lobe including hippocampus in the AD compared to the CN participants. However, mGluR5 binding appears to be lower in most cortical regions. Comparison of mGluR5 binding in the hippocampus (**b**) and association cortex (**c**) between AD and CN participants. AD participants—compared to CN participants—demonstrated significantly lower overall mGluR5 binding ($F(1, 31) = 7.4, p = 0.011$). In addition, there was a significant diagnostic group \times region interaction ($F(1, 31) = 9.2, p = 0.0049$). Post hoc analyses revealed that hippocampal mGluR5 binding ($p = 0.003, t$ test), but not association cortical mGluR5 binding ($p = 0.093$), was reduced in AD participants. Error bars represent standard deviations. BP_{ND} , binding potential; CN, cognitively normal; AD, Alzheimer's disease. $*p < .05$

FreeSurfer Desikan-Killiany regions. For the surface-based analysis, there were no significant differences between AD and CN groups when a cluster-wise correction for multiple comparisons was applied. In an uncorrected surface-based analysis, the cortical pattern of mGluR5 binding in AD included significant reductions in the entorhinal cortex and posterior cingulum. There were also clusters of reduced signal throughout the cortices more broadly (Fig. 3, Additional file 1: Table S2).

For the analysis of all FreeSurfer regions, the effect size (Cohen's d) to detect a difference in BP_{ND} between AD and CN groups was calculated (Additional file 1: Figure S1). Consistent with the primary regional analyses, the largest effect sizes were found in the medial temporal lobe. Additional file 1:

Table S3 presents group differences (unpaired t tests) for all ROIs included in Additional file 1: Figure S1.

Discussion

We used PET to investigate $[^{18}\text{F}]\text{FPEB}$ binding (BP_{ND}) in early AD and observed a significant 43% reduction of mGluR5 availability in hippocampus but only a nonsignificant trend in a composite association cortical region. Exploratory analyses in a wider range of ROIs also suggested lower mGluR5 binding in the entorhinal cortex and parahippocampal gyrus. Reduction in mGluR5 availability in the hippocampus, but not entorhinal cortex or parahippocampal gyrus, remained significant after corrections for GM atrophy and partial volume effects. Additional exploratory analyses

Table 2 mGluR5 binding ($[^{18}\text{F}]\text{FPEB } BP_{\text{ND}}$) in exploratory brain regions of interest

Exploratory regions	Cognitively normal	Alzheimer's disease	p value
	Mean BP_{ND} (SD)	Mean BP_{ND} (SD)	
Prefrontal cortex	1.89 (0.65)	1.64 (0.25)	0.155
Entorhinal cortex	1.62 (0.46)	1.07 (0.45)	0.002*
Parahippocampal gyrus	1.52 (0.48)	1.13 (0.32)	0.012*
Lateral temporal cortex	1.94 (0.64)	1.59 (0.27)	0.060
Lateral parietal cortex	1.80 (0.59)	1.50 (0.29)	0.077
Posterior cingulum	0.99 (0.61)	0.79 (0.25)	0.230
Precuneus	1.77 (0.57)	1.50 (0.26)	0.094
Occipital cortex	1.67 (0.53)	1.44 (0.21)	0.113
Caudate	1.26 (0.72)	1.07 (0.51)	0.391
Putamen	2.16 (0.77)	1.96 (0.30)	0.326
Thalamus	0.90 (0.50)	0.64 (0.25)	0.080

Data are mean (SD). BP_{ND} binding potential of $[^{18}\text{F}]\text{FPEB}$ in regions of interest. Cognitively normal ($n = 15$), Alzheimer's disease ($n = 16$). p values are for post hoc two-tailed, unpaired t tests (uncorrected for multiplicity) performed after a linear mixed model analysis of BP_{ND} in multiple regions (within-subject factor) between CN and AD diagnostic groups

* $p < .05$

suggested that hippocampal mGluR5 binding was associated with episodic memory performance and inversely associated with global function (CDR-SB) in the overall sample.

Comparison with AD model mouse and postmortem human studies

This is the first investigation of mGluR5 availability in living AD subjects. Previous studies of mGluR5 expression have

been limited to mouse models of AD and a single small post-mortem report. Fang et al. investigated changes in mGluR5 expression in A β PP transgenic mice (tg-ArcSwe) with ex vivo immunoblotting and in vivo $[^{11}\text{C}]\text{ABP688}$ -PET imaging. Immunoblot assays showed that brain mGluR5 levels tended to be upregulated in tg-ArcSwe mice compared with wild-type mice, although these changes were not discernible with PET [17]. By contrast, Lee et al. measured mGluR5

Table 3 mGluR5 binding ($[^{18}\text{F}]\text{FPEB } BP_{\text{ND}}$) in brain regions of interest

	BP_{ND} —gray matter masked			BP_{ND} —partial volume corrected		
	CN, mean (SD)	AD, mean (SD)	p	CN, mean (SD)	AD, mean (SD)	p
Primary region						
Hippocampus	1.78 (0.61)	1.30 (0.33)	0.011*	2.69 (0.88)	2.19 (0.45)	0.0499*
Composite association cortex	2.38 (0.76)	2.04 (0.29)	0.111	4.39 (1.30)	3.99 (0.47)	0.258
Exploratory regions						
Prefrontal cortex	2.43 (0.78)	2.15 (0.29)	0.197	4.48 (1.34)	4.10 (0.49)	0.310
Entorhinal cortex	1.99 (0.72)	1.52 (0.43)	0.034*	3.18 (1.18)	2.69 (0.54)	0.144
Parahippocampal gyrus	1.96 (0.69)	1.58 (0.33)	0.052	3.26 (1.13)	2.86 (0.44)	0.199
Lateral temporal cortex	2.43 (0.81)	2.03 (0.31)	0.075	4.24 (1.34)	3.78 (0.45)	0.204
Lateral parietal cortex	2.32 (0.72)	1.97 (0.31)	0.091	4.44 (1.26)	4.01 (0.52)	0.211
Posterior cingulum	1.65 (0.64)	1.42 (0.30)	0.219	3.23 (1.05)	3.01 (0.45)	0.448
Precuneus	2.15 (0.66)	1.82 (0.27)	0.079	4.08 (1.16)	3.71 (0.47)	0.249
Occipital cortex	2.02 (0.59)	1.77 (0.25)	0.120	3.82 (1.03)	3.57 (0.41)	0.388
Caudate	2.17 (0.86)	1.98 (0.42)	0.439	3.41 (1.26)	3.14 (0.46)	0.427
Putamen	2.79 (0.91)	2.57 (0.35)	0.381	4.44 (1.37)	4.19 (0.64)	0.514
Pallidum	0.96 (0.41)	0.81 (0.42)	0.312	2.50 (1.18)	2.30 (0.83)	0.599
Thalamus	1.38 (0.61)	1.12 (0.27)	0.118	2.40 (0.91)	2.04 (0.41)	0.162

Data are mean (SD). BP_{ND} binding potential of $[^{18}\text{F}]\text{FPEB}$ in regions of interest, CN cognitively normal ($n = 15$), AD Alzheimer's disease ($n = 16$). p values are for post hoc two-tailed, unpaired t tests (uncorrected for multiplicity) performed after a linear mixed model analysis of BP_{ND} in multiple regions (within-subject factor) between CN and AD diagnostic groups

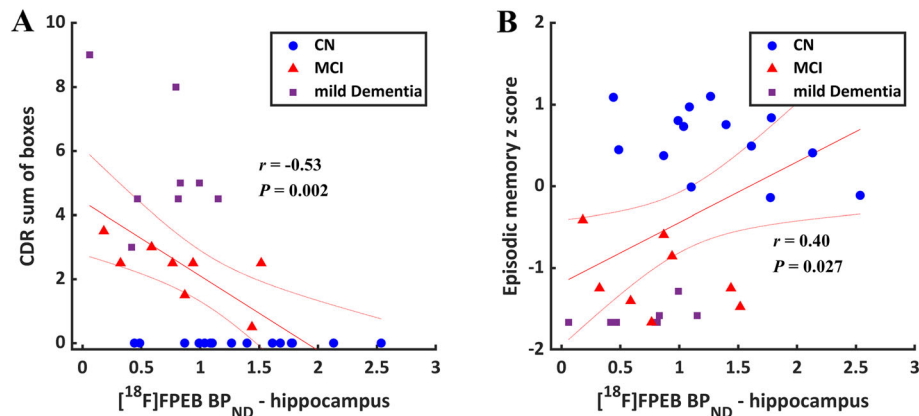


Fig. 2 Association of mGluR5 binding ($[^{18}\text{F}]\text{FPEB } BP_{\text{ND}}$) in the hippocampus with Clinical Dementia Rating (CDR) sum of boxes and episodic memory. Reduced hippocampal mGluR5 binding was associated with more severe disease ($r = -0.53$, $p = 0.002$) measured by CDR sum of boxes (a) and lower composite episodic memory scores (b) ($r = 0.40$, $p = 0.027$) in the overall sample. Episodic memory performance is the average of z-scores for CVLT free delayed recall and Logical Memory II. The figure displays linear regression line with its 95% confidence interval. CDR, Clinical Dementia Rating

density in 5xFAD mice using $[^{18}\text{F}]\text{FPEB}$ -PET and immunoblot and observed lower mGluR5 binding and protein levels in the hippocampus and striatum compared to wild-type mice [18]. The reasons for these divergent findings in mouse models of AD are unclear. However, 5xFAD mice recapitulate more features of AD, including loss of neurons and a reduction of several synaptic markers [42], which may explain the greater similarity to our results with $[^{18}\text{F}]\text{FPEB}$ -PET in human AD. The only postmortem study of mGluR5 binding in AD by Müller Herde et al. [43] utilized $[^{18}\text{F}]\text{PSS232}$ autoradiography and reported increases in the frontal cortex (5.2-fold) and hippocampus (2.5-fold) in 6 patients with severe AD compared to 6 controls. The authors speculate that neuroinflammation may lead to mGluR5 upregulation in severe

AD and note that these results may not apply to early-stage AD, which may indeed explain the discrepancy with our results using $[^{18}\text{F}]\text{FPEB}$ -PET. However, further postmortem and in vivo research at different stages of AD will be necessary to elucidate these issues.

Relevance for AD pathogenesis

The significance of reduced hippocampal $[^{18}\text{F}]\text{FPEB}$ binding in early AD is unclear. Hippocampal reductions in mGluR5 may simply be the product of nonspecific synaptic loss, which would explain the similarity of these results (43% reduction in hippocampal BP_{ND}) with our recent findings with the synaptic PET tracer $[^{11}\text{C}]\text{UCB-J}$ in a comparable early AD sample [21]. That study

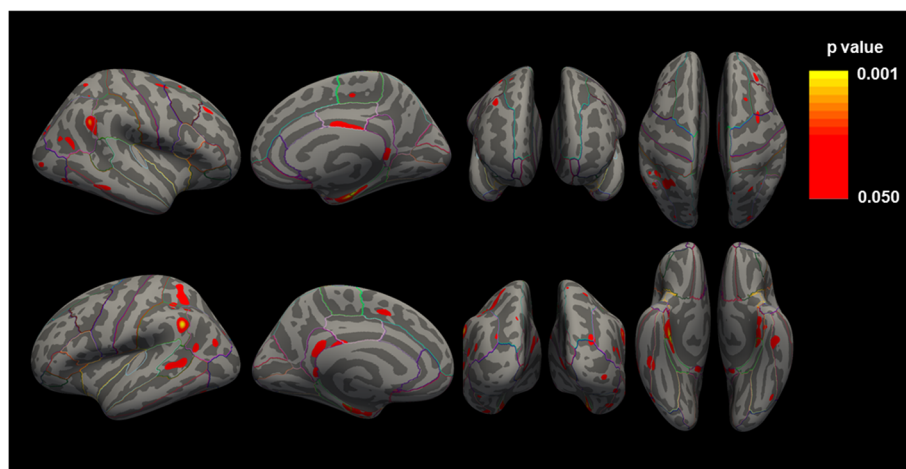


Fig. 3 Whole cortex comparison of mGluR5 binding ($[^{18}\text{F}]\text{FPEB } BP_{\text{ND}}$) between AD and CN groups. p values are for vertex-wise comparisons between AD and CN groups uncorrected for multiple comparisons and thresholded at $p < .05$. Significant vertices are represented in pseudocolor. All displayed clusters are for the contrast CN > AD. BP_{ND} , binding potential; CN, cognitively normal; AD, Alzheimer's disease

demonstrated a 41% reduction in hippocampal BP_{ND} , consistent with postmortem reports of hippocampal synaptic loss in MCI and mild AD [19, 20]. Alternatively, the presence of mGluR5 may influence the regional pattern of synaptic loss, given the evidence for involvement of this receptor in AD pathogenesis. mGluR5 has been hypothesized to mediate A β o synaptotoxicity by a number of mechanisms, including promoting the clustering of A β o as an extracellular scaffold for mGluR5 [9] and serving as a co-receptor for A β o bound to PrP^c for post-synaptic activation of the tyrosine kinase Fyn [11, 44]. If A β o synaptotoxicity occurs preferentially at mGluR5 sites, then this might also account for the synaptic pattern of mGluR5 reductions in the present study. Multitracer PET imaging studies with [¹⁸F]FPEB and [¹¹C]UCB-J may be able to dissociate the regional pattern of mGluR5 and synaptic losses in early AD.

Corrections for brain atrophy

We have presented mGluR5 binding results for [¹⁸F]FPEB-PET both with and without correction for AD-related decreases in regional brain volumes. We calculated the BP_{ND} for AAL-derived ROIs and repeated this calculation using a GM mask [30]. Finally, we performed PVC with the Müller-Gärtner algorithm to correct for GM signal loss (spill-out) due to atrophy [30, 33]. PVC typically has its greatest impact in those ROIs with large differences in GM volume between AD and CN groups (Additional file 1: Table S1) where spill-out could falsely lower BP_{ND} . As expected, values of BP_{ND} increased with application of these correction methods (Table 2 and Table 3), but group differences in hippocampal mGluR5 binding remained significant—albeit with decreased magnitude. Our results suggest that lower hippocampal mGluR5 binding in AD is driven partly by a loss of GM volume but that a decrease in receptor density is also present in the remaining tissue. Among the outcome measures presented, the optimal one may depend on the particular purpose. Uncorrected analyses have greater sensitivity when mGluR5 imaging is utilized as a biomarker of disease presence or progression and may introduce less measurement error. This measure also summarizes the net loss of mGluR5, i.e., a combination of tissue loss and loss of mGluR5 in the remaining tissue. Corrections for GM loss and partial volume effects are better suited to determine group differences in receptor concentrations and may permit comparison to in vitro studies using animal models and postmortem human brain tissue.

Assumptions and limitations of mGluR5 receptor quantification with BP_{ND}

In this study, we quantified [¹⁸F]FPEB binding to mGluR5 using BP_{ND} generated from equilibrium modeling [36]

with whole cerebellum as the reference region. We have previously evaluated a bolus plus constant infusion paradigm for equilibrium modeling of V_T and BP_{ND} for [¹⁸F]FPEB [31, 37, 38] and demonstrated excellent test-retest reproducibility for both parameters [31]. A major strength of BP_{ND} over V_T —particularly for an older, AD population—is that it does not require arterial or venous blood sampling and is less susceptible to errors in the input function [28, 40]. The major limitation of BP_{ND} for mGluR5 quantification with [¹⁸F]FPEB is that it assumes a validated reference region with negligible specific binding. Although cerebellum is the region with the least mGluR5 specific binding, a small but measurable mGluR5 signal is observed in human cerebellum [33]. This will cause BP_{ND} values to be underestimated and the magnitude of percent group differences to be overestimated. Nonetheless, the estimation of BP_{ND} using a region with a small amount of specific binding may be useful with certain assumptions—in particular, that specific binding in the reference region does not differ between diagnostic groups. Importantly, we observed no significant difference in cerebellar V_T (reflecting specific plus nonspecific binding) between AD and CN groups.

Conclusion

We observed reduced hippocampal mGluR5 binding with [¹⁸F]FPEB-PET in early AD compared to CN participants. Exploratory analyses suggested that these reductions may extend to other medial temporal lobe structures. Further study is needed to define the regional pattern and temporal course of mGluR5 alterations in AD, as well as the associations with cognitive and functional status. Quantification of [¹⁸F]FPEB binding to mGluR5 in AD may expand our understanding of AD pathogenesis and aid in the development of novel biomarkers and treatments.

Supplementary information

Supplementary information accompanies this paper at <https://doi.org/10.1186/s13195-020-0582-0>.

Additional file 1: Supplemental Methods. Description of AAL regions use to construct composite ROIs. **Table S1.** Gray Matter Volume (cm³) in brain regions of interest. Gray matter volume comparison in AD and CN groups. **Table S2A.** Left hemisphere surface-based analysis of mGluR5 binding. List of freesurfer ROI group differences in the left hemisphere. **Table S2B.** Right hemisphere surface-based analysis of mGluR5 binding. List of freesurfer ROI group differences in the right hemisphere. **Figure S1.** Effect size maps of [¹⁸F]FPEB binding (BP_{ND}) to mGluR5 in AD compared to CN participants. **Table S3.** mGluR5 binding in all FreeSurfer regions.

Abbreviations

AAL: Automated anatomical labeling; AD: Alzheimer's disease; A β o: Amyloid- β oligomer; tg-ArcSwe: A β PP transgenic mice; BP_{ND} : Binding potential; PIB: Pittsburgh Compound B; CDR: Clinical Dementia Rating; CN: Cognitively normal; CSF: Cerebrospinal fluid; DVR: Distribution volume ratio; GM: Gray matter; LMI: Logical Memory II; MCI: Mild cognitive impairment;

mGluR5: Metabotropic glutamate subtype 5 receptor; MMSE: Mini-Mental Status Examination; MPRAGE: Magnetization-prepared rapid gradient-echo; MRI: Magnetic resonance imaging; PET: Positron emission tomography; PrP^C: Cellular prion protein; PVC: Partial volume correction; RAVLT: Rey Auditory Verbal Learning Test; ROI: Region of interest; V_r: Distribution volume; WM: White matter

Acknowledgements

We wish to thank staff of the Yale PET Center for their excellent technical assistance and Brent Vander Wyk, Ph.D., for his review of the statistical analysis plan.

Authors' contributions

APM, REC, SMS, and CHV contributed to the study concept and design. APM, JWM, HRM, TAG, JEH, MKC, AS, NBN, KL, YH, REC, SMS, and CHV contributed to the acquisition, analysis, or interpretation of the data, as well as critical revision of the manuscript for important intellectual content. APM, REC, and CHV performed the statistical analysis. APM, REC, CHV, and SMS obtained the funding. APM, MKC, AS, NBN, KL, YH, REC, SMS, and CHV provided administrative, technical, or material support. All authors read and approved the final manuscript.

Funding

This research was supported by the National Institute on Aging (P50-AG047270 and K23-AG057784) and National Institute of Mental Health (R25-MH071584). The funding bodies had no role in the design of the study, data collection, analysis, interpretation, or writing of the manuscript.

Availability of data and materials

The datasets used and/or analyzed during the current study are not publicly available due to ongoing analysis and manuscript preparation but are available from the corresponding author on reasonable request.

Ethics approval and consent to participate

The study protocol was approved by the Yale University Human Investigation Committee and Radiation Safety Committee. All participants provided written informed consent prior to participating in the study.

Consent for publication

Not applicable

Competing interests

The authors declare that they have no competing interests.

Author details

¹Alzheimer's Disease Research Unit, Yale University School of Medicine, One Church Street, 8th Floor, New Haven, CT 06510, USA. ²Department of Psychiatry, Yale University School of Medicine, New Haven, CT, USA. ³Department of Neuroscience, Yale University School of Medicine, New Haven, CT, USA. ⁴Department of Neurology, Yale University School of Medicine, New Haven, CT, USA. ⁵Department of Radiology and Biomedical Imaging, Yale University School of Medicine, New Haven, CT, USA. ⁶CNNR Program, Yale University School of Medicine, 295 Congress Avenue, Ste 431-435, New Haven, CT, USA.

Received: 21 July 2019 Accepted: 5 January 2020

Published online: 18 January 2020

References

- Awad H, Hubert GW, Smith Y, Levey AI, Conn PJ. Activation of metabotropic glutamate receptor 5 has direct excitatory effects and potentiates NMDA receptor currents in neurons of the subthalamic nucleus. *J Neurosci*. 2000; 20(21):7871–9.
- Abushik PA, Niitykoski M, Giniatullina R, Shakirzyanova A, Bart G, Fayuk D, et al. The role of NMDA and mGluR5 receptors in calcium mobilization and neurotoxicity of homocysteine in trigeminal and cortical neurons and glial cells. *J Neurochem*. 2014;129(2):264–74.
- Daggett LP, Sacaan AI, Akong M, Rao SP, Hess SD, Liaw C, et al. Molecular and functional characterization of recombinant human metabotropic glutamate receptor subtype 5. *Neuropharmacology*. 1995;34(8):871–86.
- Ohnuma T, Augood SJ, Arai H, McKenna PJ, Emson PC. Expression of the human excitatory amino acid transporter 2 and metabotropic glutamate receptors 3 and 5 in the prefrontal cortex from normal individuals and patients with schizophrenia. *Brain Res Mol Brain Res*. 1998;56(1–2):207–17.
- Shigemoto R, Kinoshita A, Wada E, Nomura S, Ohishi H, Takada M, et al. Differential presynaptic localization of metabotropic glutamate receptor subtypes in the rat hippocampus. *J Neurosci*. 1997;17(19):7503–22.
- Shigemoto R, Nomura S, Ohishi H, Sugihara H, Nakanishi S, Mizuno N. Immunohistochemical localization of a metabotropic glutamate receptor, mGluR5, in the rat brain. *Neurosci Lett*. 1993;163(1):53–7.
- Gereau RW, Conn PJ. Multiple presynaptic metabotropic glutamate receptors modulate excitatory and inhibitory synaptic transmission in hippocampal area CA1. *J Neurosci*. 1995;15(10):6879–89.
- Muly EC, Maddox M, Smith Y. Distribution of mGluR1alpha and mGluR5 immunolabeling in primate prefrontal cortex. *J Comp Neurol*. 2003;467(4):521–35.
- Renner M, Lacor PN, Velasco PT, Xu J, Contractor A, Klein WL, et al. Deleterious effects of amyloid beta oligomers acting as an extracellular scaffold for mGluR5. *Neuron*. 2010;66(5):739–54.
- Um JW, Kaufman AC, Kostylev M, Heiss JK, Stagi M, Takahashi H, et al. Metabotropic glutamate receptor 5 is a coreceptor for Alzheimer abeta oligomer bound to cellular prion protein. *Neuron*. 2013;79(5):887–902.
- Haas LT, Salazar SV, Kostylev MA, Um JW, Kaufman AC, Strittmatter SM. Metabotropic glutamate receptor 5 couples cellular prion protein to intracellular signalling in Alzheimer's disease. *Brain*. 2016;139(Pt 2):526–46.
- Nygaard HB, van Dyck CH, Strittmatter SM. Fyn kinase inhibition as a novel therapy for Alzheimer's disease. *Alzheimers Res Ther*. 2014;6(1):8.
- Kostylev MA, Tuttle MD, Lee S, Klein LE, Takahashi H, Cox TO, et al. Liquid and hydrogel phases of PrP(C) linked to conformation shifts and triggered by Alzheimer's amyloid-beta oligomers. *Mol Cell*. 2018;72(3):426–43 e12.
- Larson M, Sherman MA, Amar F, Nuvolone M, Schneider JA, Bennett DA, et al. The complex PrP(c)-Fyn couples human oligomeric Abeta with pathological tau changes in Alzheimer's disease. *J Neurosci*. 2012;32(47):16857–71a.
- Iltner LM, Ke YD, Delerue F, Bi M, Gladbach A, van Eersel J, et al. Dendritic function of tau mediates amyloid-beta toxicity in Alzheimer's disease mouse models. *Cell*. 2010;142(3):387–97.
- Haas LT, Salazar SV, Smith LM, Zhao HR, Cox TO, Herber CS, et al. Silent allosteric modulation of mGluR5 maintains glutamate signaling while rescuing Alzheimer's mouse phenotypes. *Cell Rep*. 2017;20(1):76–88.
- Fang XT, Eriksson J, Antoni G, Yngve U, Cato L, Lannfelt L, et al. Brain mGluR5 in mice with amyloid beta pathology studied with in vivo [11C]ABP688 PET imaging and ex vivo immunoblotting. *Neuropharmacology*. 2017;113(Pt A):293–300.
- Lee M, Lee HJ, Park IS, Park JA, Kwon YJ, Ryu YH, et al. Aβ pathology downregulates brain mGluR5 density in a mouse model of Alzheimer. *Neuropharmacology*. 2018;133:512–7.
- Scheff SW, Price DA, Schmitt FA, DeKosky ST, Mufson EJ. Synaptic alterations in CA1 in mild Alzheimer disease and mild cognitive impairment. *Neurology*. 2007;68(18):1501–8.
- Scheff SW, Price DA, Schmitt FA, Mufson EJ. Hippocampal synaptic loss in early Alzheimer's disease and mild cognitive impairment. *Neurobiol Aging*. 2006;27(10):1372–84.
- Chen MK, Mecca AP, Naganawa M, Finnema SJ, Toyonaga T, Lin SF, et al. Assessing synaptic density in Alzheimer disease with synaptic vesicle glycoprotein 2A positron emission tomographic imaging. *JAMA neurology*. 2018;75(10):1215–24.
- Braak H, Alafuzoff I, Arzberger T, Kretzschmar H, Del Tredici K. Staging of Alzheimer disease-associated neurofibrillary pathology using paraffin sections and immunocytochemistry. *Acta Neuropathol*. 2006;112(4):389–404.
- Giannakopoulos P, Hof PR, Bouras C. Selective vulnerability of neocortical association areas in Alzheimer's disease. *Microsc Res Tech*. 1998;43(1):16–23.
- MKhann GM, Knopman DS, Chertkow H, Hyman BT, Jack CR Jr, Kawas CH, et al. The diagnosis of dementia due to Alzheimer's disease: recommendations from the National Institute on Aging-Alzheimer's Association workgroups on diagnostic guidelines for Alzheimer's disease. *Alzheimers Dement*. 2011;7(3):263–9.
- Albert MS, DeKosky ST, Dickson D, Dubois B, Feldman HH, Fox NC, et al. The diagnosis of mild cognitive impairment due to Alzheimer's disease: recommendations from the National Institute on Aging-Alzheimer's Association workgroups on diagnostic guidelines for Alzheimer's disease. *Alzheimers Dement*. 2011;7(3):270–9.
- Reiman E, Chen K, Liu X, Bandy D, Yu M, Lee W, et al. Fibrillar amyloid-β burden in cognitively normal people at 3 levels of genetic risk for Alzheimer's disease. *Proc Natl Acad Sci U S A*. 2009;106(16):6820–5.

27. de Jong HW, van Velden FH, Kloet RW, Buijs FL, Boellaard R, Lammertsma AA. Performance evaluation of the ECAT HRRT: an LSO-LYSO double layer high resolution, high sensitivity scanner. *Phys Med Biol*. 2007;52(5):1505–26.
28. Carson RE, Barker W, Liow J-S, Adler S, Johnson C. Design of a motion-compensation OSEM list-mode algorithm for resolution-recovery reconstruction of the HRRT. *IEEE Nucl Sci Symp Conf Rec*. 2003:M16–6.
29. Jin X, Mulnix T, Gallezot JD, Carson RE. Evaluation of motion correction methods in human brain PET imaging—a simulation study based on human motion data. *Med Phys*. 2013;40(10):102503.
30. Mecca AP, Barcelos NM, Wang S, Bruck A, Nabulsi N, Planeta-Wilson B, et al. Cortical beta-amyloid burden, gray matter, and memory in adults at varying APOE epsilon4 risk for Alzheimer's disease. *Neurobiol Aging*. 2017;61:207–14.
31. Park E, Sullivan JM, Planeta B, Gallezot JD, Lim K, Lin SF, et al. Test-retest reproducibility of the metabotropic glutamate receptor 5 ligand [(1)(8) F] FPEB with bolus plus constant infusion in humans. *Eur J Nucl Med Mol Imaging*. 2015;42(10):1530–41.
32. Tzourio-Mazoyer N, Landeau B, Papathanassiou D, Crivello F, Etard O, Delcroix N, et al. Automated anatomical labeling of activations in SPM using a macroscopic anatomical parcellation of the MNI MRI single-subject brain. *Neuroimage*. 2002;15(1):273–89.
33. Müller-Gärtner HW, Links JM, Prince JL, Bryan RN, McVeigh E, Leal JP, et al. Measurement of radiotracer concentration in brain gray matter using positron emission tomography: MRI-based correction for partial volume effects. *J Cereb Blood Flow Metab*. 1992;12(4):571–83.
34. Innis RB, Cunningham VJ, Delforge J, Fujita M, Gjedde A, Gunn RN, et al. Consensus nomenclature for in vivo imaging of reversibly binding radioligands. *J Cereb Blood Flow Metab*. 2007;27(9):1533–9.
35. Wu Y, Carson RE. Noise reduction in the simplified reference tissue model for neuroreceptor functional imaging. *J Cereb Blood Flow Metab*. 2002;22:1440–52.
36. Carson RE, Channing MA, Blasberg RG, Dunn BB, Cohen RM, Rice KC, et al. Comparison of bolus and infusion methods for receptor quantitation: application to [18F] cyclofoxy and positron emission tomography. *J Cereb Blood Flow Metab*. 1993;13(1):24–42.
37. Abdallah CG, Hannestad J, Mason GF, Holmes SE, DellaGioia N, Sanacora G, et al. Metabotropic glutamate receptor 5 and glutamate involvement in major depressive disorder: a multimodal imaging study. *Biol Psychiatry Cogn Neurosci Neuroimaging*. 2017;2(5):449–56.
38. Sullivan JM, Lim K, Labaree D, Lin SF, McCarthy TJ, Seibyl JP, et al. Kinetic analysis of the metabotropic glutamate subtype 5 tracer [(18) F] FPEB in bolus and bolus-plus-constant-infusion studies in humans. *J Cereb Blood Flow Metab*. 2013;33(4):532–41.
39. Patel S, Hamill TG, Connolly B, Jagoda E, Li W, Gibson RE. Species differences in mGluR5 binding sites in mammalian central nervous system determined using in vitro binding with [18F]F-PFB. *Nucl Med Biol*. 2007; 34(8):1009–17.
40. Fischl B. *FreeSurfer Neuroimage*. 2012;62(2):774–81.
41. Buckner RL, Head D, Parker J, Fotenos AF, Marcus D, Morris JC, et al. A unified approach for morphometric and functional data analysis in young, old, and demented adults using automated atlas-based head size normalization: reliability and validation against manual measurement of total intracranial volume. *Neuroimage*. 2004;23(2):724–38.
42. Oakley H, Cole SL, Logan S, Maus E, Shao P, Craft J, et al. Intraneuronal beta-amyloid aggregates, neurodegeneration, and neuron loss in transgenic mice with five familial Alzheimer's disease mutations: potential factors in amyloid plaque formation. *J Neurosci*. 2006;26(40):10129–40.
43. Müller Herde A, Schibli R, Weber M, Ametamey SM. Metabotropic glutamate receptor subtype 5 is altered in LPS-induced murine neuroinflammation model and in the brains of AD and ALS patients. *Eur J Nucl Med Mol Imaging*. 2018;46(2):407–420.
44. Um JW, Strittmatter SM. Amyloid-beta induced signaling by cellular prion protein and Fyn kinase in Alzheimer disease. *Prion*. 2013;7(1):37–41.

Publisher's Note

Springer Nature remains neutral with regard to jurisdictional claims in published maps and institutional affiliations.

Ready to submit your research? Choose BMC and benefit from:

- fast, convenient online submission
- thorough peer review by experienced researchers in your field
- rapid publication on acceptance
- support for research data, including large and complex data types
- gold Open Access which fosters wider collaboration and increased citations
- maximum visibility for your research: over 100M website views per year

At BMC, research is always in progress.

Learn more biomedcentral.com/submissions

